OsteoArthritis and Cartilage (2005) **13,** 418–425

doi:10.1016/j.joca.2004.12.011

Osteoarthritis and Cartilage

International Cartilage Repair Society

OARSI OSTEOARTHRITIS RESEARCH SOCIETY INTERNATIONAL

Degenerative knee joint disease in mice lacking 3′-phosphoadenosine 5′-phosphosulfate synthetase 2 (Papss2) activity: a putative model of human *PAPSS2* deficiency-associated arthrosis[1]

Alice F. Ford-Hutchinson B.Sc.†, Zenobia Ali Ph.D.†, Ruth A. Seerattan‡, David M. L. Cooper M.Sc.§, Benedikt Hallgrímsson Ph.D., Associate Professor‖, Paul T. Salo M.D., F.R.C.S.C., Associate Professor‡ and Frank R. Jirik M.D., F.R.C.P.C., Professor†*

† *Department of Biochemistry and Molecular Biology, The McCaig Center for Joint Injury and Arthritis Research, University of Calgary, Calgary, Alberta, T2N 4N1, Canada*

‡ *Department of Surgery, The McCaig Center for Joint Injury and Arthritis Research, University of Calgary, Calgary, Alberta, T2N 4N1, Canada*

§ *Department of Archaeology and Medical Science, The McCaig Center for Joint Injury and Arthritis Research, University of Calgary, Calgary, Alberta, T2N 4N1, Canada*

‖ *Department of Cell Biology and Anatomy, The McCaig Center for Joint Injury and Arthritis Research, University of Calgary, Calgary, Alberta, T2N 4N1, Canada*

Summary

Objective: Murine brachymorphism (*bm*) results from an autosomal recessive mutation of the *Papss2* gene that encodes 3′-phosphoadenosine 5′-phosphosulfate synthetase 2, one of the principal enzymes required for the sulfation of extracellular matrix molecules in cartilage and other tissues. A spondyloepimetaphyseal dysplasia has been identified in Pakistani kindred having a mutation of *PAPSS2*. In addition to skeletal malformations that include short stature evident at birth due to limb shortening, brachydactyly, and kyphoscoliosis [Ahmad M, Haque MF, Ahmad W, Abbas H, Haque S, Krakow D, *et al*. Distinct, autosomal recessive form of spondyloepimetaphyseal dysplasia segregating in an inbred Pakistani kindred. Am J Med Genet 1998;78:468–73], affected individuals demonstrate premature onset degenerative joint disease. We investigated whether loss of Papss2 activity would similarly lead to degenerative joint disease in mice.

Methods: Mice carrying the *bm* mutation on a C57BL/6 background were obtained from the Jackson Laboratory. Limbs were analyzed by micro-computed tomography (μCT) and histology.

Results: At 12 months of age both male and female *bm* mice exhibited severe degenerative knee joint disease, with cartilage damage being primarily evident in the patello-femoral and medial compartments. Control 12–14-month-old C57BL/6 mice, in contrast, only occasionally demonstrated minimal cartilage damage. μCT imaging of *bm* limbs revealed shortened diaphyses associated with flared metaphyses in the proximal elements of both fore and hind limbs. Additionally, the *bm* hind limbs demonstrated extensive structural alterations, characterized by distortion of the patello-femoral groove, and prominent bowing of both tibia and fibula.

Conclusions: The *bm* mutant, which develops severe articular cartilage lesions of the knee joint by approximately 12 months of age, represents a novel example of murine degenerative joint disease, possibly representing a model of human *PAPSS2* deficiency-associated arthrosis.

Key words: Degenerative joint disease, PAPSS2, Micro-computed tomography, Brachymorph.

Introduction

Murine brachymorphism (*bm*) results from an autosomal recessive mutation of one of the genes (*Papss2*) encoding 3′-phosphoadenosine 5′-phosphosulfate synthetase 2[1–5], an enzyme required for sulfation reactions on a variety of different substrates. Papss2 is a bi-functional enzyme, having both adenosine triphosphate (ATP)-sulfurylase and adenosine-5′-phosphosulfate (APS)-kinase activities. After sulfate import into the cell, this molecule is converted (by reaction with ATP) into the 'high energy' species, phosphoadenosine-phosphosulfate (PAPS). PAPS is subsequently translocated into the Golgi where the sulfate groups are transferred, by a sulfotransferase, onto a variety of different recipient molecules. Sulfate group addition is important in

[1] *Support*: This work was supported by a Canadian Institutes of Health Research grant (to FRJ); FRJ held Alberta Heritage Foundation for Medical Research (AHFMR) Medical Scientist and Canada Research Chair awards; and AFF-H was the recipient of an AHFMR studentship award. Acquisition of the micro-computed tomography system was enabled by grants from the Canada Foundation for Innovation (3923) and Alberta Innovation and Science (#URSI-01-103-RI) (to BH).

*Address correspondence and reprint requests to: Dr Frank Jirik, 3330 Hospital Drive N.W., Calgary, Alberta, Canada T2N 4N1. Tel: 1-403-220-8666; Fax: 1-403-210-8127; E-mail: jirik@ucalgary.ca

Received 23 July 2004; revision accepted 20 December 2004.

many contexts, including, the deactivation or activation of xenobiotics, hormone (e.g., catecholamine) inactivation, elimination of specific end-products of catabolism, and in maintaining both the structure and function of extracellular matrix (ECM) macromolecules[6]. With respect to the latter, one of the key substrates of sulfation reactions are the glycosaminoglycans (GAGs)[1,7], disaccharide units that are covalently linked to the core proteins of proteoglycans.

The *Papss2* defect in brachymorphic mice results from a point mutation causing a Gly to Arg substitution within a highly-conserved region of the APS kinase domain that greatly impairs enzymatic activity[5]. Although *bm/bm* cartilage contains normal levels of GAGs, these are hyposulfated[1,2,7], and as a result, less negatively charged than the GAGs of control cartilage[2]. Although *bm/bm* mouse cartilage matrix contained normal collagen fibrils, proteoglycans aggregate granules were smaller and reduced in number as compared to control mice, particularly in the columnar and hypertrophic zones of the growth plate[7]. It has also been suggested that premature mineralization may occur in the *bm/bm* mice given that hyposulfated proteoglycans are less effective at inhibiting hydroxyapatite deposition[8,9].

The *bm/bm* mouse phenotype is characterized by foreshortened limbs, a short stout tail, and a complex craniofacial phenotype (responsible for the characteristic dome-shaped cranium of these mutant mice) whose origin remains to be fully elucidated. Despite these abnormalities, *bm/bm* mice are fertile, and have normal life-spans[10]. Consistent with the role of the Papss2 in sulfate donation, *bm/bm* mice exhibit abnormal hepatic detoxification of specific chemicals, increased bleeding times (attributed to platelet dysfunction), and diminished postnatal growth due to epiphyseal growth plate disruption. The latter results in *bm/bm* limbs being ~50% shorter than control limbs by 4 weeks of age, and axial skeleton length being reduced by ~25%.

Recently, a novel form of spondyloepimetaphyseal dysplasia (SEMD) was reported in a Pakistani kindred, that was associated with a truncation mutation of the human *PAPSS2* gene[11,12]. Affected individuals exhibited various skeletal malformations, including short stature (already evident at birth), short bowed lower limbs (*genu varum*), mild brachydactyly, and kyphoscoliosis[11]. They also exhibited early onset of an osteoarthritis-like degenerative disease in various joints, including knees, hands, and spine.

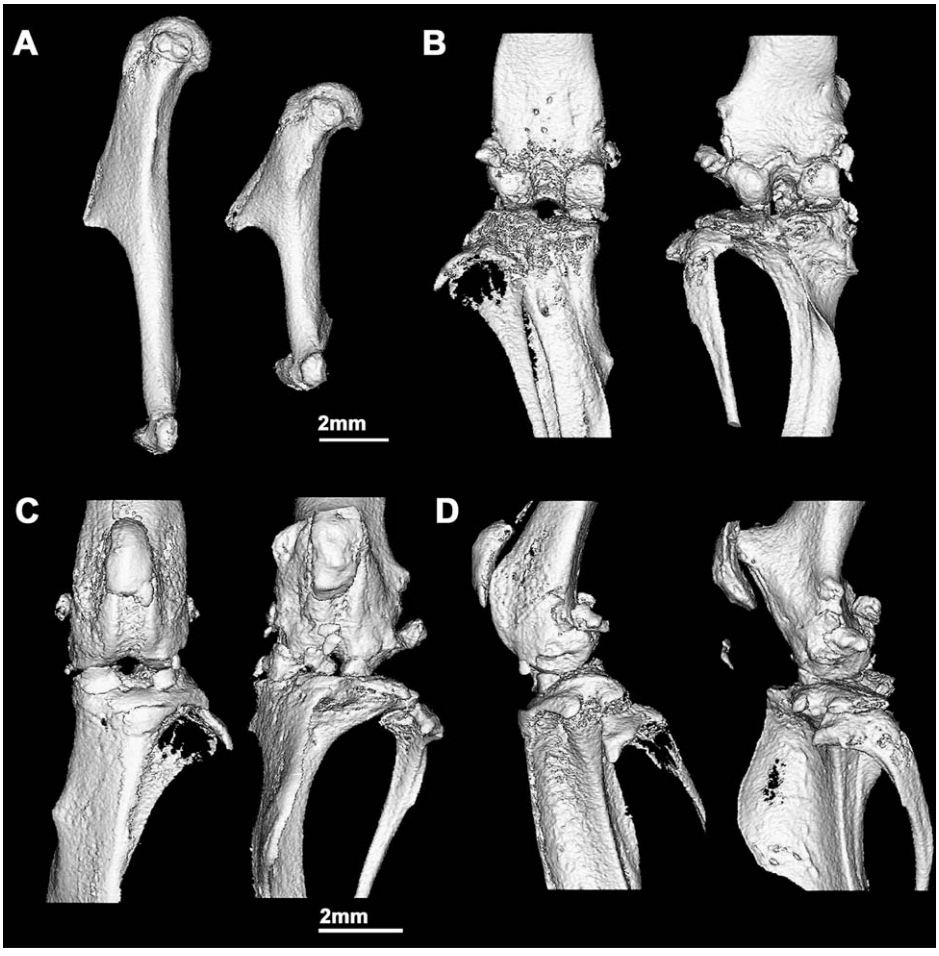

Fig. 1. 3D reconstruction of left humeri and knees from representative 12-month-old normal (left) and *bm/bm* (right) mice. The image of the humeri (A) illustrates the distinctive limb morphology of the *bm/bm* mutant. Also shown are posterior (B), anterior (C), and lateral (D) views of the knees: bowing of the tibia is seen in the *bm/bm* mice (B, C) compared to controls; and the enlarged, anteriorly-displaced patellar groove (with overlying patella), as well as the excessive growth of the tibial tuberosity resulting in a fin-like structure in the *bm/bm* sample, are best seen in panel D.

Although degenerative joint disease had not been previously reported, we hypothesized that brachymorph mice would also show cartilage pathology with age.

Materials and methods

ANIMALS

Mice homozygous for the *Papss2* gene mutation, *bm/bm*, on a C57BL/6 background were obtained from Jackson Laboratories (Bar Harbor, ME, USA). Six C57BL/6 control mice (three males and three females) were examined at 12–14 months of age, and four (one male and three females) at 6–9 months. Six *bm/bm* mice (three males and three females) were examined at 12 months, and three at 6–7 months of age (two males and one female). Mice were maintained in a barrier facility in accord with University of Calgary Animal Care Committee and Canadian Council on Animal Care guidelines, and euthanized by CO_2 inhalation. Limbs to be scanned were removed at the level of the hip and shoulder. Following dissection, limbs to be examined by histology were immediately placed in 10% neutral buffered formalin for fixation and then processed for histological examination. Skeletal samples to be examined by micro-computed tomography (μCT) were stored at −20°C. We have established that cryopreservation does not alter the morphology of skeletal samples for μCT.

μCT ANALYSIS

Intact limbs were scanned using a Skyscan 107 (Aartselaar, Belgium) as described in Ford-Hutchinson *et al.*[13]. Two isotropic scan resolutions, 15, and 5 μm, were used for the visualization of gross limb morphology, and morphometric analysis of proximal tibial subchondral plates, respectively. Three-dimensional (3D) volumetric renderings were produced using Analyze 5.0 (AnalyzeDirect, Lenexa, KS). Software provided with scanner was used to measure the 3D thickness distributions of the tibial plateaus, using a model-independent method[14]. The proximal articular surfaces of the tibia were segmented manually prior to morphometric analysis using the same software.

HISTOLOGY

Hind limbs were transected 1 cm above and below the knee joint line, fixed in 10% neutral buffered formalin (Fisher Scientific) for 7 d and then decalcified in either Cal Ex, or Cal Ex II (Fisher Scientific), for 10–14 d at room temperature, with daily changes of the solution. Following decalcification, joints were thoroughly rinsed with water, dehydrated, cleared and then infiltrated using an automatic processor (Autotechnicon Mono 2A). Paraffin wax-embedded tissue blocks were cut (8 μm serial sagittal sections) and mounted on glass slides, with every other slide being sequentially stained with hematoxylin, fast green, and safranin-O (VWR), and mounted with Permount (Fisher).

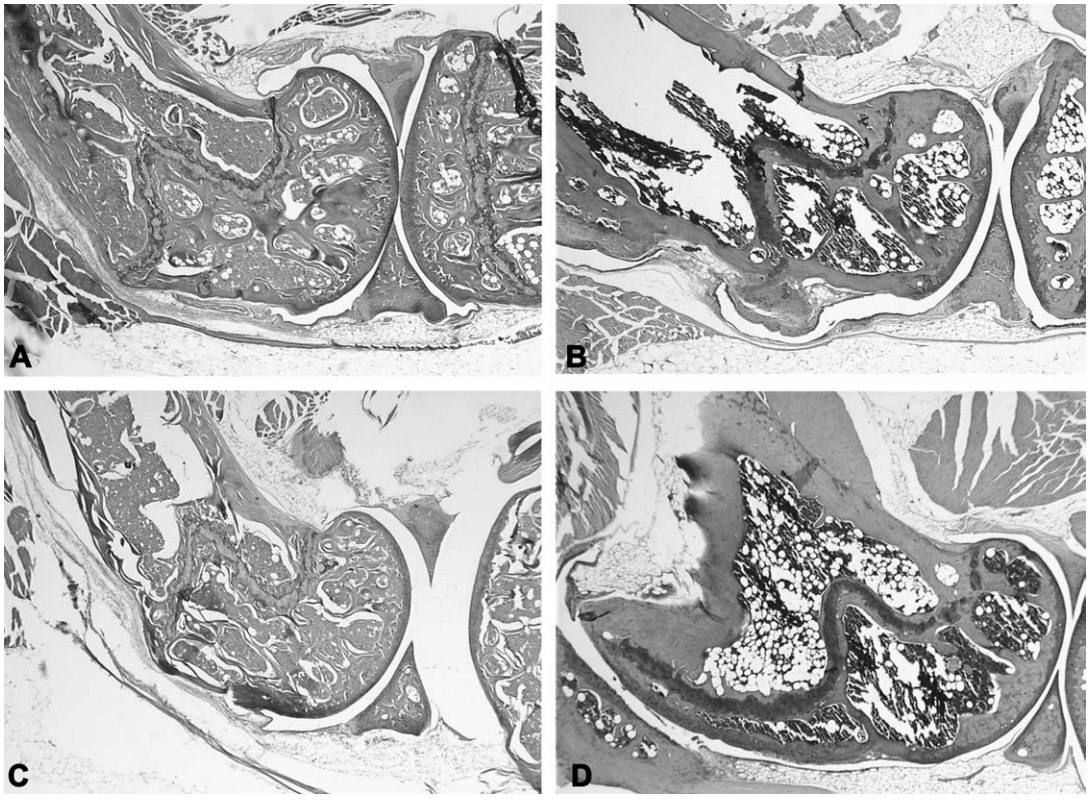

Fig. 2. Matched pairs of sagittal sections taken through the femoral condyles of representative 12-month-old control (A, C) and *bm/bm* (B, D) mice. A and B illustrate the medial compartments, C and D the patello-femoral compartments of the knees. Note the altered, hammer head-like (inverted in this image) shape of the distal femur in the *bm/bm* mouse (D) which correlates with the changes seen in the μCT scan [Fig. 1(D)].

The complete set of serial alternate sections of each knee joint was examined on a Leitz DMRB microscope (Leica). Joints were individually assessed by the grading system of Maier and Wilhelmi[15], with scoring based on a scale of 0–4, with 4 being the most severe. Statistical analysis was performed using a Mann–Whitney (Wilcoxon) test.

Results

μCT ANALYSIS OF *BM/BM* LIMBS

Volumetric 3D renderings, based upon the μCT data, revealed striking morphological differences between wild-type and *bm/bm* limbs. In general, the bones of the *bm/bm* mice appeared more robust due to their reduced diaphyseal lengths and relatively enlarged epiphyses. This is illustrated in the humeri shown in Fig. 1(A). Along with this diaphyseal shortening, metaphyseal flaring was a distinctive characteristic of *bm/bm* long bones. In the femur, for example, this flaring was associated with a pronounced change in the shape of the distal epiphysis, associated with an extensive alteration in the configuration of the patello-femoral groove that resulted in the distal femurs having a hammer head-like shape [Fig. 1(D)]. This alteration was also clearly evident in histological sections of the distal *bm/bm* femur, as seen in Fig. 2(D). Additional changes in *bm/bm* limbs included enlarged muscle and tendon insertion points, as seen in the deltoid [Fig. 1(A)] and tibial [Fig. 1(D)] tuberosities. Bowing of the tibia and fibula [Fig. 1(B–D)] was also present, as was evidence of abnormal radiodensities about the knee (osteophytosis) and irregularities of menisci in *bm/bm* samples. The abnormal morphology of the distal femur was also evident histologically [Fig. 2(B, D)]. We compared proximal tibial subchondral plate thicknesses between wild-type and *bm/bm* tibiae to search for the possibility of an abnormality in subchondral bone structure, but found no significant difference (*bm* = 122 μm, wild-type = 119, *t* test, two tailed, $P = 0.7$).

HISTOLOGICAL ANALYSIS OF *BM/BM* KNEE JOINTS

While the synovial lining of control of 6–7-month C57BL/6 mice was approximately 1–2 cells thick [Fig. 3(A)], the lining of brachymorph knees appeared thickened and hypercellular [Fig. 3(B)]. The same was observed for our 12–14-month knees (data not shown). The significance of this synovial hypertrophy is unclear, but suggests the presence of a chronic low-grade inflammation. In control mice, the narrow yet well-organized epiphyseal growth plates were consistent with slowed growth of long bones. These plates showed a columnar organization of cells and an organized progression from proliferating to hypertrophic cells [Fig. 3(C)]. As previously reported, the growth plates of *bm/bm* mice were abnormal, lacking the regular columnar organization of proliferating and hypertrophying chondrocytes of C57BL/6 mice [Fig. 3(D)]. Indeed, in the *bm/bm* samples there was no clear distinction between the different zones of the growth plate, with these tending to collapse into disorganized, often round, clumps of cells. The epiphyseal growth plates of the 12-month-old *bm/bm* also appeared less cellular than those of controls and showed evidence of impaired

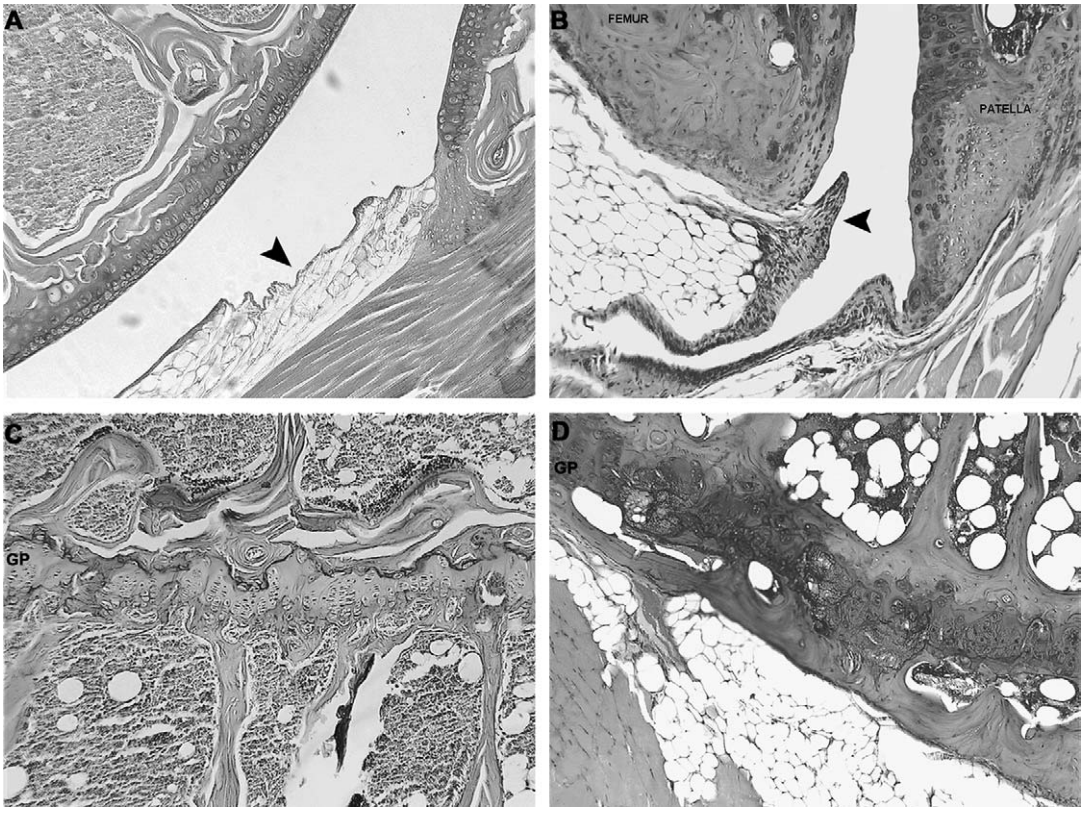

Fig. 3. Synovial lining of control (A) and *bm/bm* (B) mice at 6–9 months of age. Note the thickened synovium in B as indicated by arrows compared to the control (A). Representative growth plates of control (C) and *bm/bm* (D) mice at 6–9 months of age.

endochondral ossification, with accumulation of mineralized cartilage matrix.

Knee joints of 6–9-month-old C57BL/6 mice exhibited histologically normal articular cartilage with regularly distributed and densely packed chondrocytes on all joint surfaces [Fig. 4(A)]. At 12–14 months, all knee joints isolated from C57BL/6 mice showed some areas of superficial fibrillation in the medial joint compartment, and occasional fraying, typically on the tibiae but also on femoral condyles [Fig. 4(B)]. This was consistent with the age-related cartilage degeneration (grade 1) seen in this inbred strain.

At 6–7 months of age, *bm/bm* knee joints showed normal appearing articular cartilage in all joint compartments, although all samples exhibited some degree of fraying or shredding of the thin central portions of the menisci [Fig. 4(C)]. Simple or complex tears of the medial meniscus were seen in all brachymorph joints obtained from 12-month-old animals [Fig. 4(D)]. At 12 months of age, degenerative changes were evident in the medial and/or patello-femoral compartments of all mutant mouse samples (Fig. 5). All *bm/bm* mice exhibited degradation of the articular cartilage on medial tibial plateaus [Fig. 5(A, B)], although the opposing femoral cartilage remained intact in most cases. Fragmentation and loss of tissue down to the level of the tidemark was seen in half the *bm/bm* animals [Fig. 5(A, B)]; with the remainder showing either horizontal ruptures along the tidemark, considered a precursor to cartilage loss (data not shown), or deep fibrillations (data not shown). The patello-femoral compartment was irregular in all brachymorph mice and half the joints had erosions on the patella and/or femur [Fig. 5(C, D)]. Interestingly, despite the advanced degenerative changes in the patello-femoral and medial joint compartments, the lateral compartments consistently presented a normal appearance (data not shown). Applying the grading system of Maier and Wilhelmi[15], the 12-month-old C57BL/6 knees had a mean score of 1.2, while the score for *bm/bm* mice was 2.5 (Table I). A Mann–Whitney (Wilcoxon) test was performed where $U = 3.45$, $P < 0.001$. It was thus concluded that the *bm/bm* mutation on a C57BL/6 background was associated with premature degenerative joint disease.

Discussion

Although the cartilage of brachymorph mice is reported to be undersulfated, normal amounts of GAGs and matrix collagens are apparently present[7,16]. Vanky *et al.*[9], have shown that this undersulfation leads to changes in the epiphyseal growth plate cartilage, leading to impaired longitudinal growth. Interestingly, changes in the sulfation of proteoglycans has also been observed within osteoarthritic joints, although this phenomenon is primarily due to enzymatic degradation and depletion of matrix GAGs, rather than hyposulfation[17,18]. In addition to an alteration in the physical properties of hyposulfated ECM molecules that may result in instability, a decreased ability of

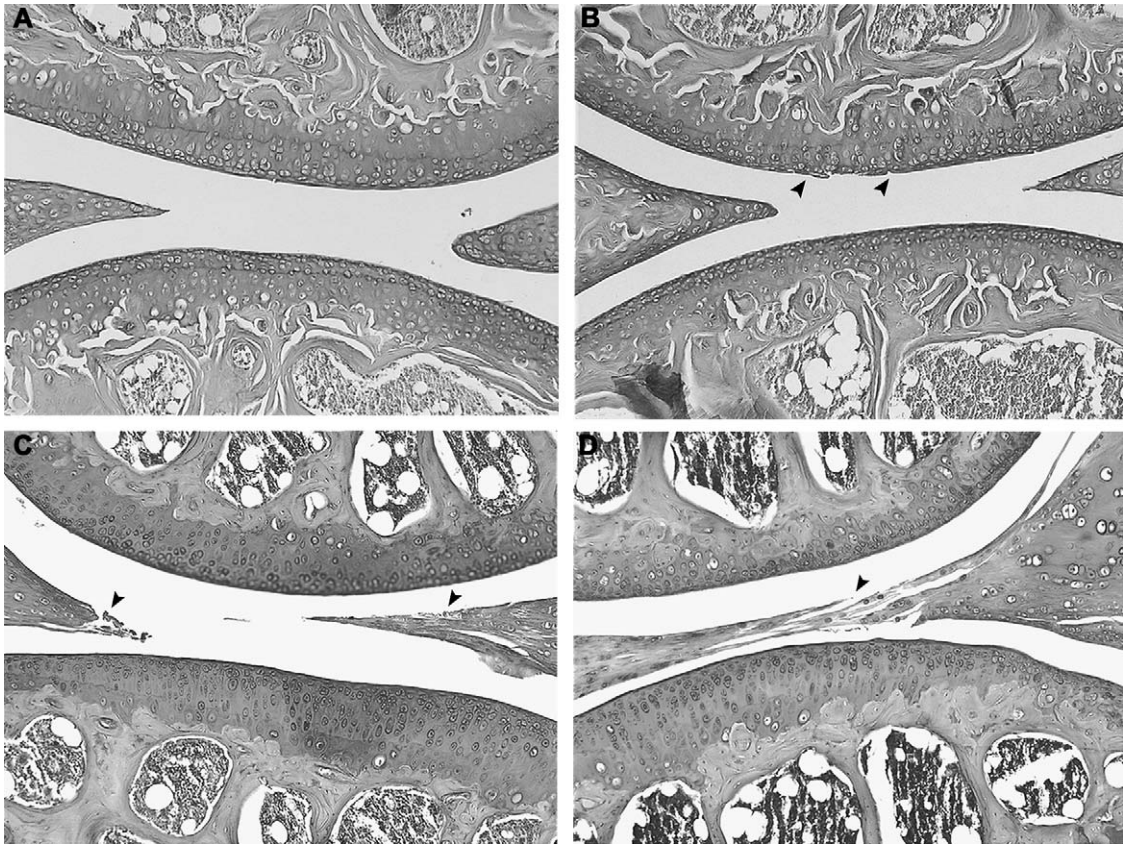

Fig. 4. Sagittal section of representative C57BL/6 control (A, B) and *bm/bm* mice (C, D). Six month (A) and 12-month-old (B) control mice. Minor fibrillation of condylar cartilage is seen in (B) (see arrows). Meniscal fraying can be seen in the 6-month-old knee (C) and, more pronounced, in a representative 12-month-old (D) knee (see arrows).

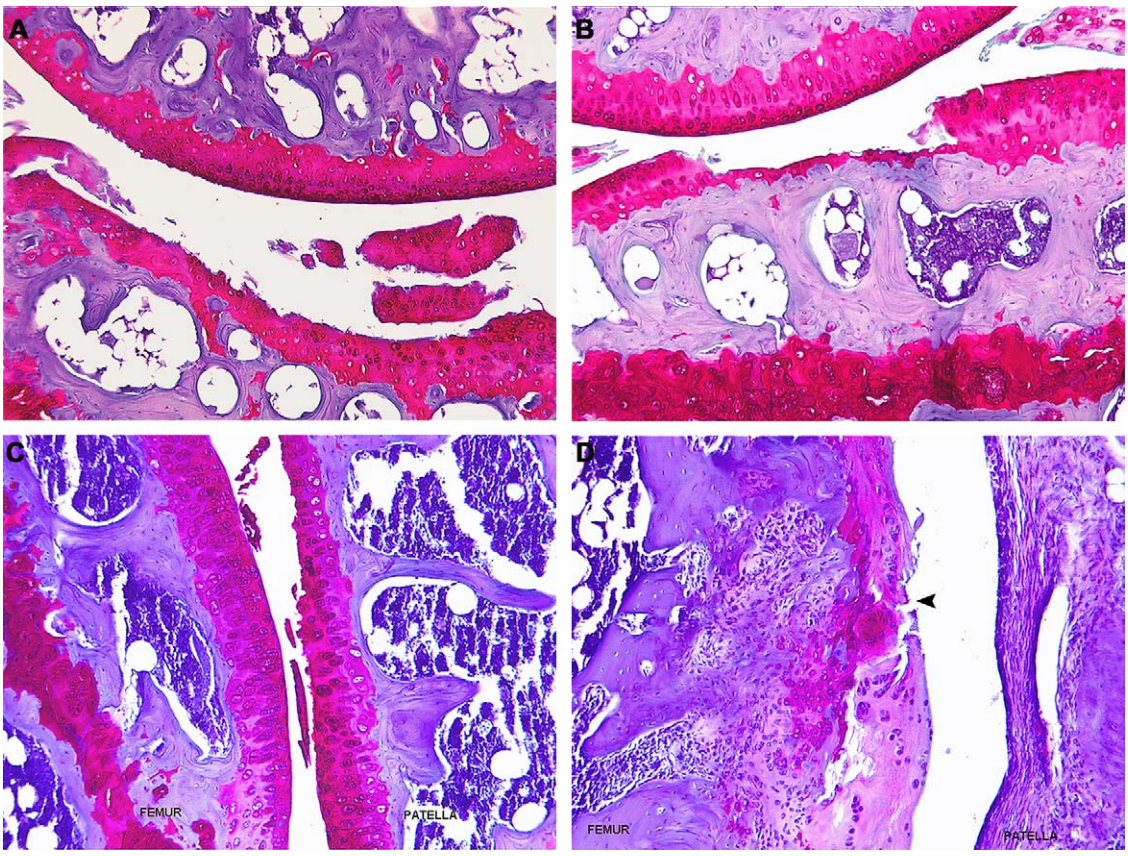

Fig. 5. Sagittal sections of representative 12-month-old *bm* knees. Medial compartment shows grade 2 and 3 changes in the articular cartilage (A, B). The grade 3 changes in (A) reveals a loss of a large area of articular cartilage right down to the tidemark, grade 2 changes are depicted in (B). Patello-femoral compartments showing surface damage of the articular cartilage (C) and deep fissuring of the cartilage (D) on the femoral side of this joint as illustrated by arrow.

proteoglycans (such as syndecans which are involved in ligand binding[19], decorin, and biglycan[20]) to present growth factors alters the growth, maintenance, and repair of articular cartilage.

The abnormalities of the ECM in all likelihood contribute to the degenerative changes seen in the articular cartilage of 12-month-old *bm* mice. ECM is supported through a network of collagen fibrils that are highly organized and stabilized via both inter- and intra-molecular cross links[21]. These resist the swelling pressure due to the negatively charged aggregates of aggrecan[22]. These negative charges, mainly due to chondroitin, are important in maintaining the structure of proteoglycans aggregates[23]. Loss of these charges, as seen in Papss2 deficiency, may cause structural instability in addition to insufficient water attraction and movement within the ECM, both leading to weakness and or instability of load-bearing joints. This would be predicted to render the articular cartilage more susceptible to damage and thence to premature degenerative joint disease.

Taken together, such factors as abnormal growth factor ligand binding and proteoglycan structure could readily account for the cartilage degeneration observed in *bm/bm* mouse knees. Other mouse models of degenerative joint disease attributed to instabilities in the ECM, include mice expressing truncated collagen type II transgene[24] and the collagen type IX knockout[25] where an alteration in the structural integrity of cartilage results from loss of a major cross-linking collagen.

Spontaneous degenerative knee joint disease has been observed in the C57BL/6 strain. Thus, with age (after 15.5 months) enlargement of menisci as well as narrowing of the joint space has been observed[26,27]. Histological evidence of cartilage destruction as early as 6–8 months of age has been reported, albeit with slow progression, whereby 80% of mice examined showed signs at 16–18 months, and almost all mice showed signs at 2 years[28]. However, the reported changes were confined primarily to the lateral side of the tibio-femoral compartment[29]. The *bm* mice, on the other hand, consistently exhibited high-grade cartilage damage at an earlier age (12 months) in both the patello-femoral and medial compartments of the knee. In addition, *bm* animals developed cartilage damage much earlier and of much greater severity than the C57BL/6 mice (Table I). The C57BL/6 mice in our control group most likely exhibited the types of changes that tend to occur spontaneously in the C57BL/6 mouse strain. Therefore, we conclude that the characteristic changes seen in all the 12-month-old *bm/bm* mice we examined were due to the loss of *Papss2* and were not a feature of the C57BL/6 genetic background.

Abnormal biomechanical function of the knee joint, as a consequence of altered morphology of the skeletal elements, may have also played a role in degeneration of the articular cartilage in *bm/bm* knees. Metaphyseal flaring and abnormal epiphyseal morphology observed in brachy-morph mouse, are also characteristic of many dysplasias resulting in dwarfism in humans[30,31]. The flaring in the

Table I
Comparison of control and bm/bm *OA grades*

Control		*bm/bm*	
Mouse	Score	Mouse	Score
1	1	7	2
2	1	8	2
3	1	9	2
4	1	10	3
5	1	11	3
6	2	12	3
Mean	1.2		2.5

Control mice include three males and three females 12−14 month C57BL/6 mice. *bm/bm* mice consisted of three males and three females 12-month-old mice. 6−9-month C57Bl/6 and *bm* were also examined (data not shown) and found to have a score of 0. A Mann−Whitney (Wilcoxon) test was performed where $U = 3.45$, $P < 0.001$.

metaphyseal region can be attributed to the capacity for normal appositional growth in the diaphysis to occur while endochondral ossification in the physis is inhibited. The epiphyseal growth plate of the *bm/bm* mice lacks the organization seen in the control mice at all ages. This finding is in agreement with other reports[9,32]. Vanky *et al.*[9] found that the chondrocytes in the proliferating zone are in the G_0 phase of the cell cycle which would result in a decrease in the number of hypertrophic cells. This paucity of hypertrophic cells was confirmed by our observations in the epiphyseal growth plate of *bm/bm* mice[9]. Although we made no attempt to identify abnormal joint kinematics or gait disturbance in the mutant mice, the skeletal abnormalities that we observed very likely resulted in abnormal contact forces in the patello-femoral and medial compartments.

Precocious development of degenerative joint disease has been associated with human chondrodystrophies[33]. With respect to the *bm/bm* mice, the various morphological alterations observed, including the bowing of the tibia and fibula, and the enlargement of muscle attachments such as the tibial and deltoid tuberosities, plausibly reflect adaptive attempts to compensate for the abnormal and disproportionate bone growth. These features might to some extent also reflect a "muscle packing" problem in that the *bm/bm* mice must accommodate muscles with similar cross-sectional areas to support the nearly normal sized trunk within a context of dramatically shortened limbs. The increased bowing of long bones, altered sites of muscle attachment relative to lever components, and the altered ratio of joint surface area to long bone length could conspire to produce dramatically altered joint mechanics. Such changes, in turn, might contribute to cartilage degeneration due to abnormal strain patterns.

Might polymorphisms of the human *PAPSS2* gene have a role in predisposition to human osteoarthritis? Xu *et al.*[34], examined a sample population and found different polymorphisms both within and outside of conserved regions of the *PAPSS2* gene, some of which could alter enzymatic activity. Thus, a mutation causing hyposulfation of proteoglycans could potentially be used as an indicator of disease predisposition. However, a study of *PAPSS2* genes in a Japanese population revealed no correlation between those affected with knee osteoarthritis[35]. It remains possible that a *PAPPS2* polymorphism(s) in a different ethnic population will be associated with susceptibility to osteoarthritis. In keeping with this, a form of human SEMD has been attributed to a mutation the *PAPSS2* gene that results in a truncated protein due to premature nonsense codon. This results in a protein that is predicted to be reduced from 614 to 437 amino acids in length[12]. It is still unknown as to whether this causes the transcript to be destabilized or whether the truncated protein retains partial activity[12]. Similarities between the human disease and the *bm/bm* model have been noted by ul Haque *et al.*[12]. Of most interest to our study is that humans lacking normal *PAPSS2* activity exhibit long bone shortening and bowing, and also show degenerative joint disease, including evidence of knee joint arthrosis. In the human SEMD families, radiographic abnormalities of the hands and spine were also observed[11]. It would be of interest to examine the spines of older *bm/bm* mice to search for evidence of degeneration. Given the premature development of degenerative knee joint disease in the mutant mice and other similarities with the human SEMD kindred, we propose that this mutant represents a model of human *PAPSS2* deficiency-associated arthrosis.

Acknowledgments

We are grateful to S. McDonogh and J. Giesbrecht for maintenance of the mouse colonies.

References

1. Schwartz NB, Ostrowski V, Brown KS, Pratt RM. Defective PAPS-synthesis in epiphyseal cartilage from brachymorphic mice. Biochem Biophys Res Commun 1978;82:173−8.
2. Sugahara K, Schwartz NB. Defect in 3′-phosphoadenosine 5′-phosphosulfate formation in brachymorphic mice. Proc Natl Acad Sci U S A 1979;76:6615−8.
3. Sugahara K, Schwartz NB. Defect in 3′-phosphoadenosine 5′-phosphosulfate synthesis in brachymorphic mice. II. Tissue distribution of the defect. Arch Biochem Biophys 1982;214:602−9.
4. Sugahara K, Schwartz NB. Defect in 3′-phosphoadenosine 5′-phosphosulfate synthesis in brachymorphic mice. I. Characterization of the defect. Arch Biochem Biophys 1982;214:589−601.
5. Kurima K, Warman ML, Krishnan S, Domowicz M, Krueger RC, Jr, Deyrup A, *et al.* A member of a family of sulfate-activating enzymes causes murine brachymorphism. Proc Natl Acad Sci U S A 1998;95:8681−5.
6. Klaassen CD, Boles JW. Sulfation and sulfotransferases 5: the importance of 3′-phosphoadenosine 5′-phosphosulfate (PAPS) in the regulation of sulfation. FASEB J 1997;11:404−18.
7. Orkin RW, Pratt RM, Martin GR. Undersulfated chondroitin sulfate in the cartilage matrix of brachymorphic mice. Dev Biol 1976;50:82−94.
8. Boskey AL, Maresca M, Wikstrom B, Hjerpe A. Hydroxyapatite formation in the presence of proteoglycans of reduced sulfate content: studies in the brachymorphic mouse. Calcif Tissue Int 1991;49:389−93.
9. Vanky P, Brockstedt U, Nurminen M, Wikstrom B, Hjerpe A. Growth parameters in the epiphyseal cartilage of brachymorphic (bm/bm) mice. Calcif Tissue Int 2000;66:355−62.
10. Orkin RW, Williams BR, Cranley RE, Poppke DC, Brown KS. Defects in the cartilaginous growth

plates of brachymorphic mice. J Cell Biol 1977;73: 287–99.
11. Ahmad M, Haque MF, Ahmad W, Abbas H, Haque S, Krakow D, *et al*. Distinct, autosomal recessive form of spondyloepimetaphyseal dysplasia segregating in an inbred Pakistani kindred. Am J Med Genet 1998;78: 468–73.
12. ul Haque MF, King LM, Krakow D, Cantor RM, Rusiniak ME, Swank RT, *et al*. Mutations in orthologous genes in human spondyloepimetaphyseal dysplasia and the brachymorphic mouse. Nat Genet 1998;20:157–62.
13. Ford-Hutchinson AF, Cooper DML, Hallgrímsson B, Jirik FR. Imaging Skeletal Pathology in Mutant Mice by Microcomputed Tomography. J Rheumatol 2003;30: 2659–65.
14. Hildebrand T, Ruegsegger P. A new method for the model independent assessment of thickness in three dimensional images. J Microsc 1997;185:67–75.
15. Maier R, Wilhelmi G. Osteoarthrosis-like disease in mice: anti-arthrotic and antirheumatic agents in mice. In: Lott DJ, Jasani MK, Birdwood GFB, Eds. Studies in Osteoarthritis: Pathogenesis, Intervention and Assessment. New York: John Wiley and Sons 1987; 75–83.
16. Pennypacker JP, Kimata K, Brown KS. Brachymorphic mice (bm/bm): a generalized biochemical defect expressed primarily cartilage. Dev Biol 1981;81:280–7.
17. Plaas AH, West LA, Wong-Palms S, Nelson FR. Glycosaminoglycan sulfation in human osteoarthritis. Disease-related alterations at the non-reducing termini of chondroitin and dermatan sulfate. J Biol Chem 1998;273:12642–9.
18. Bayliss MT, Howat S, Davidson C, Dudhia J. The organization of aggrecan in human articular cartilage. Evidence for age-related changes in the rate of aggregation of newly synthesized molecules. J Biol Chem 2000;275:6321–7.
19. Carey DJ. Syndecans: multifunctional cell-surface co-receptors. Biochem J 1997;327(Pt 1):1–16.
20. Hildebrand A, Romaris M, Rasmussen LM, Heinegard D, Twardzik DR, Border WA, *et al*. Interaction of the small interstitial proteoglycans biglycan, decorin and fibromodulin with transforming growth factor beta. Biochem J 1994;302(Pt 2):527–34.
21. Poole AR. In: Koopman WJ, Ed. Arthritis and Allied Conditions. Baltimore: Williams and Wilkins, 1996.
22. Sandy JD, Plaas AHK, Rosenberg LC. In: Koopman WJ, Ed. Arthritis and Allied Conditions. Baltimore: Williams and Wilkins 1996;252–75.
23. Mankin HJ, Mow VV, Buckwalter JA, Iannotti JP, Ratcliffe A. Articular cartilage structure, composition, and function. In: Buckwalter JA, Einhorn TA, Simon SR, Eds. Orthopaedic Basic Science, Biology and Biomechanics of the Musculoskeletal System. Illinois: American Academy of Orthopaedic Surgeons 2000; 444–70.
24. Saamanen AK, Salminen HJ, Dean PB, De Crombrugghe B, Vuorio EI, Metsaranta MP. Osteoarthritis-like lesions in transgenic mice harboring a small deletion mutation in type II collagen gene. Osteoarthritis Cartilage 2000;8:248–57.
25. Fassler R, Schnegelsberg PN, Dausman J, Shinya T, Muragaki Y, McCarthy MT, *et al*. Mice lacking alpha 1 (IX) collagen develop noninflammatory degenerative joint disease. Proc Natl Acad Sci U S A 1994;91: 5070–4.
26. Pataki A, Graf HP, Witzemann E. Spontaneous osteoarthritis of the knee-joint in C57BL mice receiving chronic oral treatment with NSAID's or prednisone. Agents Actions 1990;29:210–7.
27. Lapvetelainen T, Nevalainen T, Parkkinen JJ, Arokoski J, Kiraly K, Hyttinen M, *et al*. Lifelong moderate running training increases the incidence and severity of osteoarthritis in the knee joint of C57BL mice. Anat Rec 1995;242:159–65.
28. Stanescu R, Knyszynski A, Muriel MP, Stanescu V. Early lesions of the articular surface in a strain of mice with very high incidence of spontaneous osteoarthritic-like lesions. J Rheumatol 1993;20:102–10.
29. Stoop R, van der Kraan PM, Buma P, Hollander AP, Billinghurst RC, Poole AR, *et al*. Type II collagen degradation in spontaneous osteoarthritis in C57Bl/6 and BALB/c mice. Arthritis Rheum 1999;42:2381–9.
30. Edeiken J. In: Wilkins W, Ed. Roentgen Diagnosis of Diseases of Bone. Baltimore, 1981.
31. Greenfield GB. Radiology of Bone Diseases. Philadelphia: J.B. Lippincott Company 1990.
32. Wikstrom B, Gay R, Gay S, Hjerpe A, Mengarelli S, Reinholt FP, *et al*. Morphological studies of the epiphyseal growth zone in the brachymorphic (bm/bm) mouse. Virchows Arch B Cell Pathol Incl Mol Pathol 1984;47:167–76.
33. Osteoarthritis. In: Brandt KD, Doherty M, Lohmander LS, Eds. Oxford: Oxford University Press, 1998.
34. Xu ZH, Freimuth RR, Eckloff B, Wieben E, Weinshilboum RM. Human 3′-phosphoadenosine 5′-phosphosulfate synthetase 2 (PAPSS2) pharmacogenetics: gene resequencing, genetic polymorphisms and functional characterization of variant allozymes. Pharmacogenetics 2002;12:11–21.
35. Ikeda T, Mabuchi A, Fukuda A, Hiraoka H, Kawakami A, Yamamoto S, *et al*. Identification of sequence polymorphisms in two sulfation-related genes, PAPSS2 and SLC26A2, and an association analysis with knee osteoarthritis. J Hum Genet 2001;46: 538–43.